

On the chiral covariant approach to $\rho\rho$ scattering

Li-Sheng Geng*

*School of Physics and Nuclear Energy Engineering & International Research Center for Nuclei and Particles in the Cosmos
& Beijing Key Laboratory of Advanced Nuclear Materials and Physics, Beihang University, Beijing 100191, China*

Raquel Molina

Physics Department, The George Washington University, Washington, DC 20052, USA

Eulogio Oset

*Departamento de Física Teórica and IFIC, Centro Mixto Universidad de Valencia-CSIC
Institutos de Investigación de Paterna, Aptdo. 22085, 46071 Valencia, Spain*

(Dated: December 26, 2016)

We go in detail around a recent work, where improvements to make the $\rho\rho$ scattering relativistically covariant are made. The paper has a remarkable conclusion that the $J = 2$ state disappears with a potential which is much more attractive than for $J = 0$, where a bound state is found. We trace this abnormal conclusion to the fact that an “on shell” factorization of the potential is done in a region where this potential is singular and develops a large discontinuous and unphysical imaginary part. A method is developed, evaluating exactly the loops with full ρ propagators, and we show that they do not develop singularities and do not have an imaginary part below threshold. With the exact result for the loops we define an effective potential, which used with the Bethe Salpeter equation provides a state with $J = 2$ around the energy of the $f_2(1270)$. In addition, the coupling of the state to $\rho\rho$ is evaluated and we find that this coupling and the T matrix around the energy of the bound state are remarkably similar to those obtained with a drastic approximation used previously in which the q^2 terms of the propagators of the exchanged ρ mesons are dropped, once the cut off in the $\rho\rho$ loop function is tuned to reproduce the bound state at the same energy.

arXiv:1612.07871v1 [nucl-th] 23 Dec 2016

* Email: lisheng.geng@buaa.edu.cn

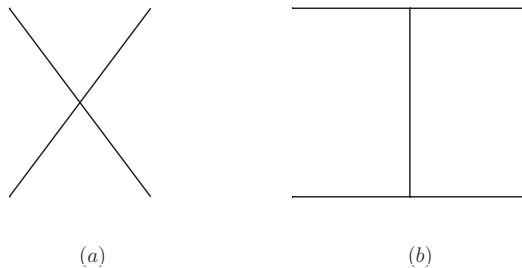


FIG. 1. Terms in the $\rho\rho$ interaction: (a) contact term; (b) ρ exchange term.

I. INTRODUCTION:

The chiral unitary approach, combining the dynamical feature of chiral Lagrangians and unitarity in coupled channels has allowed to make much progress in the meson meson [1–4] and meson baryon interactions [5–9] (see review paper [10]). One step forward in this direction was the extension of the approach to study the interaction of vector mesons among themselves. The first of such works studied the $\rho\rho$ interaction [11] which was found attractive in the isospin $I = 0$ and spin $J = 0, 2$ channels. The strength of the interaction in the $J = 2$ channel was found more than twice as big as that of the $J = 0$ channel. In both cases it was sufficient to produce bound states. The one with $J = 0$ was associated to the $f_0(1370)$ and the one with $J = 2$ to the $f_2(1270)$ states. The work was generalized to the SU(3) sector [12] and more resonant states were found that could be associated to known states.

In the works of [11, 12] the parameters of the loop function were fine tuned. With natural values of the parameters in order to find the binding at the experimental energies, the couplings of the resonances to different channels were extracted. These couplings were then used to study radiative decays [13] and other decays [14], and in all cases consistency with experiment was found.

The works of [11, 12] relied upon an approximation of neglecting the three momenta of the vector mesons with respect to their mass. This approximation was questioned in a recent work [15] where improvements were done to make a fully relativistic approach. The authors found that in the $\rho\rho$ interaction the $I = J = 0$ state, the $f_0(1370)$ was obtained, very close to the one of Ref. [11], but the $f_2(1270)$ did not appear. This is certainly surprising because if the $f_0(1370)$ appears bound, the $f_2(1270)$, where the interaction is also attractive and with a strength more than double the one in the $I = J = 0$ sector, should also appear as a bound state. In the present paper we show the reasons of the findings of Ref. [15] in the on shell factorizations of the potential, which is done on top of a singularity, generated as a consequence of this on shell factorization. The singularity does not appear in the exact loop function, which we evaluate here. We propose a different method based on the exact results for the loop function and show that in that case the $I = 0, J = 2$ channel generates a bound state, more bound than the $I = J = 0$ state. The other important finding here is that, if the parameters to regularize the loop are tuned to obtain the $f_2(1270)$ bound at the experimental energy, the coupling of the state to $\rho\rho$ is very close to the one obtained with the non relativistic approach of [11]. It is well known that for composite states, and the case of a small binding, the coupling is only tied to the binding energy [16–18]. In the case of the $f_2(1270)$ the binding is 270 MeV with respect to the nominal two ρ masses. Yet, this number is misleading because the ρ has a width of 150 MeV and with two ρ mesons their mass components go more than 300 MeV below the nominal mass and the binding is not as extreme as it seems. From this perspective it is not so surprising that we find the couplings so similar in different approaches.

II. SUMMARY OF THE $\rho\rho$ INTERACTION

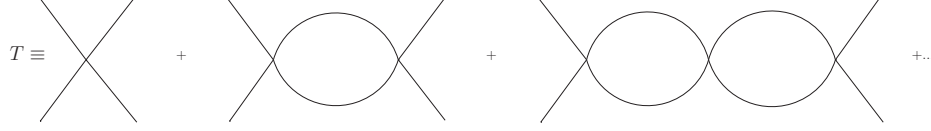
In Ref. [11] the local hidden gauge approach [19–21] was used to generate the $\rho\rho$ interaction. The formalism leads to two terms, a contact term and a ρ exchange term, which are depicted in Fig. 1,

In Ref. [11], the ρ exchange propagator was taken as $1/(-M_\rho^2)$, where the q^2 dependence of the propagator was removed. This is done in analogy to the more general case in pseudoscalar interactions where the standard lowest order chiral Lagrangians can be obtained from the local hidden gauge approach exchanging vector mesons and removing the q^2 term in the propagator. There is another approximation done in [11] since the three body vertex $\rho\rho\rho$ contains six terms and only the two leading terms were kept, neglecting terms that go like p_ρ/M_ρ . This is improved in [15]. With these approximations the interaction obtained in [11] is given in Table I, with $g = M_V/(2f)$, M_V the vector mass and f the pion decay constant $f = 93$ MeV.

One can see that the attraction in the case of $J = 2$ is much bigger than in $J = 0$. With the interaction in Table I

TABLE I. Potential, V , for the scalar and tensor channels with $I = 0$.

I	J	Contact	Exchange	Total at threshold $[I^G(J^{PC})]$
0	0	$8g^2$	$-8g^2 \left(\frac{3s}{4M_\rho^2} - 1 \right)$	$-8g^2[0^+(0^{++})]$
0	2	$-4g^2$	$-8g^2 \left(\frac{3s}{4M_\rho^2} - 1 \right)$	$-20g^2[0^+(2^{++})]$

FIG. 2. Diagrammatic representation of the $\rho\rho$ scattering matrix.

one solves the Bethe Salpeter equation,

$$T = [1 - VG]^{-1}V, \quad (1)$$

where G is the loop function of two ρ meson propagators. Since the interaction has been reduced to a constant (independent of momentum transfer) for each value of s , the square of the total mass in the $\rho\rho$ rest frame, the amplitude T in Eq. (1) is summing the diagrams of Fig. 2, and G is given in the cut off regularization by

$$G = \int_{|\vec{q}| \leq q_{\max}} \frac{d^3q}{(2\pi)^3} \frac{\omega_1 + \omega_2}{2\omega_1\omega_2[P^0]^2 - (\omega_1 + \omega_2)^2 + i\epsilon]} \quad (2)$$

where q_{\max} stands for the cutoff, $(P^0)^2 = s$ and $\omega_i = \sqrt{\vec{q}^2 + M_\rho^2}$. However, in the case of the ρ , which has a large width, one cannot neglect its mass distribution. This is very important and was taken into account in [11] by making a convolution of G over the mass distribution of the two ρ mesons as follows

$$\tilde{G}(s) = \frac{1}{N^2} \int_{(M_\rho - 2\Gamma_\rho)^2}^{(M_\rho + 2\Gamma_\rho)^2} d\tilde{m}_1^2 \left(-\frac{1}{\pi}\right) \mathcal{I}m \frac{1}{\tilde{m}_1^2 - M_\rho^2 + i\Gamma\tilde{m}_1} \times \int_{(M_\rho - 2\Gamma_\rho)^2}^{(M_\rho + 2\Gamma_\rho)^2} d\tilde{m}_2^2 \left(-\frac{1}{\pi}\right) \mathcal{I}m \frac{1}{\tilde{m}_2^2 - M_\rho^2 + i\Gamma\tilde{m}_2} G(s, \tilde{m}_1^2, \tilde{m}_2^2), \quad (3)$$

with

$$N = \int_{(M_\rho - 2\Gamma_\rho)^2}^{(M_\rho + 2\Gamma_\rho)^2} d\tilde{m}_1^2 \left(-\frac{1}{\pi}\right) \mathcal{I}m \frac{1}{\tilde{m}_1^2 - M_\rho^2 + i\Gamma\tilde{m}_1}, \quad (4)$$

where $M_\rho = 770$ MeV, $\Gamma_\rho = 146.2$ MeV and for $\Gamma \equiv \Gamma(\tilde{m})$ we take the ρ width for the decay into the pions in p -wave

$$\Gamma(\tilde{m}) = \Gamma_\rho \left(\frac{\tilde{m}^2 - 4m_\pi^2}{M_\rho^2 - 4m_\pi^2} \right)^{3/2} \theta(\tilde{m} - 2m_\pi). \quad (5)$$

The use of this \tilde{G} function gives a width to the bound states obtained from the $\rho \rightarrow \pi\pi$ decay. In addition, box diagrams with four intermediate π mesons were also considered in [11], which account for the $\pi\pi$ decay channel of the states obtained. This channel is not a matter of concern in [15] and we shall not discuss it here.

III. BEYOND THE STATIC ρ EXCHANGE WITH ON SHELL FACTORIZATION

The novelty in [15], which is the reason for the disappearance of the tensor state, stems from keeping the q^2 dependence in the ρ exchange potential in Fig. 1(b). To show that, one can still use the potential in Table I, since the relativistic improvements on the vertices have nothing to do with this problem. The ρ propagator in Fig. 1(b) gives in the notation $p_1 + p_2 \rightarrow p_3 + p_4$

$$D(\rho) = \frac{1}{q^2 - M_\rho^2 + i\epsilon} = \frac{1}{(p_1 - p_3)^2 - M_\rho^2 + i\epsilon} = \frac{1}{-2\vec{p}^2(1 - \cos\theta) - M_\rho^2 + i\epsilon} \quad (6)$$

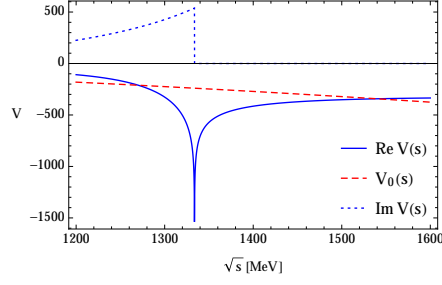


FIG. 3. Dashed line: $V_0 = V_c + V_{\text{ex}}$ from [11]. Solid line: $\text{Re } V(s)$ of Eq. (8). Dotted line: $\text{Im } V(s)$ of Eq. (8)

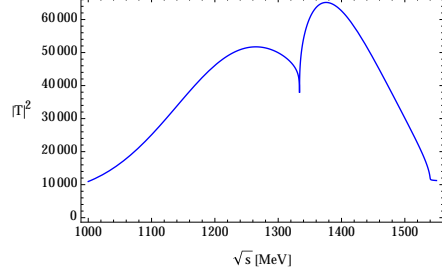


FIG. 4. The results for $|T|^2$ with the potential of Eq. (8).

where we have taken $\vec{p}_1 = p\hat{u}_z$, $\vec{p}_2 = -\vec{p}_1$, and as in [15] we have taken $q^0 = 0$. This corresponds to the on shell factorization, where the interaction V is taken for an on shell situation. The next assumption in the on shell factorization in [15] is that $p_i^2 = M_\rho^2$. Thus $p^2 = (\frac{E}{2})^2 - M_\rho^2$ and hence, p^2 becomes negative for bound states, $E = \sqrt{s} < 2M_\rho$. Here is where the problem begins because the ρ exchange develops a singularity. However, we can already advance that this singularity never appears in the loops of the Bethe Salpeter equation of Fig. 2 when the $\rho\rho\rho\rho$ vertex is substituted by the ρ exchange diagram of Fig. 1(b). Continuing with the derivation, we project the ρ -exchange in s -wave as done in [15] and we obtain

$$D_\rho(s\text{-wave}) = -\frac{1}{4p^2} \log \left(\frac{4p^2 + M_\rho^2}{M_\rho^2} + i \frac{4\rho^2\epsilon}{M_\rho^4} \right). \quad (7)$$

We can see that when $4p^2 + M_\rho^2 \equiv s - 4M_\rho^2 + M_\rho^2 = 0$, this has a singularity, and the on shell factorized potential becomes infinite at $s = 3M_\rho^2$. In addition for $s < 3M_\rho^2$, $D_\rho(s\text{-wave})$ develops an imaginary part.

In Fig. 3, we plot the new potential

$$V(s) = V_c + V_{\text{ex}} D_\rho(s\text{-wave})(-M_\rho^2) \quad (8)$$

with V_c and V_{ex} from Table I, where we have replaced $\frac{1}{-M_\rho^2}$ by $D_\rho(s\text{-wave})$ in the V_{ex} potential of [11].

As we can see, the new potential of Eq. (8) is remarkably similar to the one exhibited in Fig. 4 of [15]. It is exactly equal to the one of [11] at threshold and develops a singularity at $s = 3M_\rho^2$. One can also see that the potential develops an imaginary part for $s < 3M_\rho^2$, with a discontinuity at $s = 3M_\rho^2$. This imaginary part is not tied to any physical process, as could be the $\rho\rho$ system decaying into 2π or 4π . We should note that the singularity appears at $\sqrt{s} = 1334$ MeV and, hence, one anticipates problems to get a state at 1270 MeV, as it would correspond to the $f_2(1270)$ state. Indeed, in Fig. 4 we plot the result of $|T|^2$ for this potential. As we can see, this does not reflect a resonance at 1270 MeV with a width of 100 MeV as the experiment. In this sense, the conclusion of [15] that the tensor resonance $f_2(1270)$ does not appear with the potential of Eq. (8) is correct. The problem is that this is a clear situation where the on shell factorization cannot be done since the “on shell” potential seats on top of a singularity of the extrapolated amplitude below threshold. Actually, it is well known that the on shell factorization does not take into account the left hand cut contribution in a dispersion relation [7, 22], and in the work of [15] the on shell factorization is used precisely where one would have the contribution from the left hand cut.

Before we proceed to perform the exact integration of the loop function with the full ρ propagator (including also the q^0 dependence) let us, however, note that the singularity obtained corresponds to using a ρ mass fixed to the

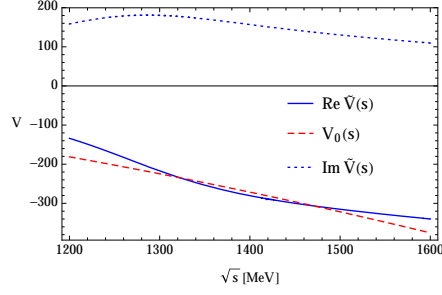
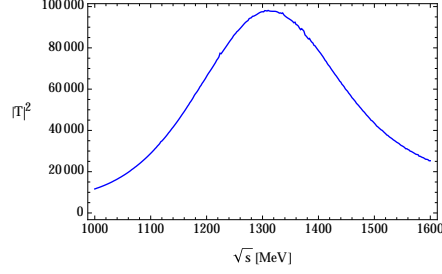


FIG. 5. The potential of Eqs. (9)(10).

FIG. 6. $|T|^2$ from $\tilde{V}(s)$ of Eqs. (9), (10) and \tilde{G} of Eq. (3) via Eq. (1).

nominal value of 770 MeV. We next show what happens if the realistic ρ mass distribution is used. For this, we take again $D_\rho(s - \text{wave})$ of Eq. (7) and make a convolution with the ρ mass distribution. Hence we use now

$$\tilde{V}(s) = V_c + V_{\text{ex}} \tilde{D}_\rho(s - \text{wave})(-M_\rho^2) \quad (9)$$

with

$$\hat{D}_\rho = \frac{1}{N} \int_{(M_\rho - 2\Gamma_\rho)^2}^{(M_\rho + 2\Gamma_\rho)^2} d\tilde{m}_\rho^2 \left(-\frac{1}{\pi} \right) \text{Im} \frac{1}{\tilde{m}_\rho^2 - M_\rho^2 + i\Gamma\tilde{m}_\rho} \left[-\frac{1}{4p^2} \log \left(\frac{4p^2 + \tilde{m}_\rho^2}{\tilde{m}_\rho^2} + i\frac{4\rho^2\epsilon}{\tilde{m}_\rho^4} \right) \right] \quad (10)$$

with N and Γ given by Eqs. (4)(5), and $p^2 = \frac{s}{2} - \tilde{m}_\rho^2$.

In Fig. (5) we show now \tilde{V}_s compared to the one of [11]. We can see that now $\tilde{V}(s)$ does not have a singularity and $\text{Re}\tilde{V}(s)$ is actually quite similar to the potential from [11]. In addition the imaginary part of $\tilde{V}(s)$ no longer has a discontinuity. It is interesting to see what happens if we use the Bethe Salpeter equation with this potential. In Fig. 6, we show $|T|^2$ evaluated with the potential $\tilde{V}(s)$ and Eq. (1) with the same cutoff $q_{\text{max}} = 875$ MeV as in [11]. Using $\tilde{G}(s)$ of Eq. (3) we see that we get a broad bump that could be identified with a resonance with mass around 1300 MeV and $\Gamma \approx 300$ MeV. So, we can see that even using the on shell approach of [15], a state with mass around 1300 MeV appears. The width however is not realistic since it is related to the imaginary part of $D_\rho(s - \text{wave})$ which is not linked to any physical channel. If we remove this spurious imaginary part, we obtain for $|T|^2$ the result shown in Fig. 7(a) which is remarkably closer to the one of [11] shown in Fig. 7(b).

IV. REALISTIC CALCULATION

In this section we are going to evaluate explicitly the loops that would appear in the Bethe Salpeter equation, Fig. (2), where a contact term or the explicit ρ exchange are used as the source of interaction. We note that at the one loop level we would have the diagrams of Fig. (8).

Next we see that around 1270 MeV we have

$$V_c = -4g^2; \quad V_{\text{ex}} = -8g^2 \frac{3s - 4M_\rho^2}{4M_\rho^2} \quad (11)$$

$$\frac{V_{\text{ex}}}{V_c} = \frac{3s - 4M_\rho^2}{2M_\rho^2} \quad (12)$$

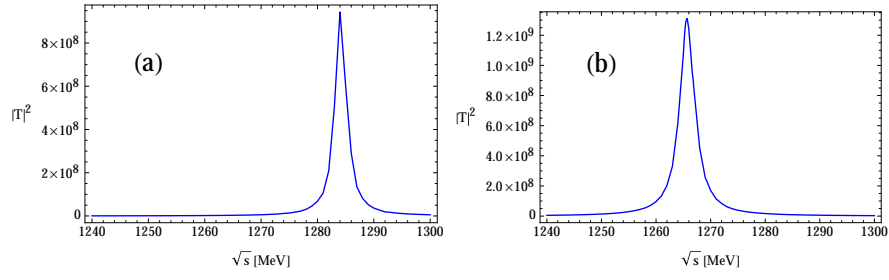


FIG. 7. $|T|^2$ obtained from $\text{Re}\tilde{V}(s)$ (a) and from $V_c + V_{\text{ex}}$ of [11] (b).

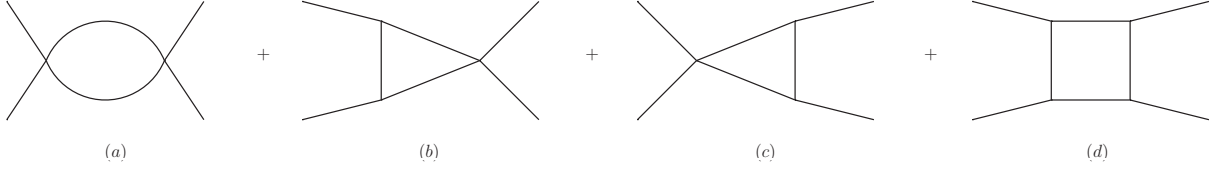


FIG. 8. Diagrams appearing at one loop level with the contact and ρ exchange terms.

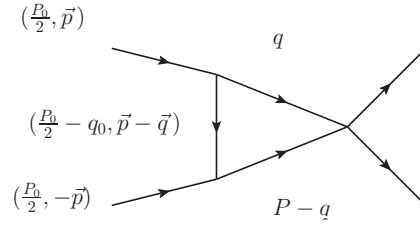


FIG. 9. Diagram of Fig. 8(b) disclosing explicitly the momenta of the particles.

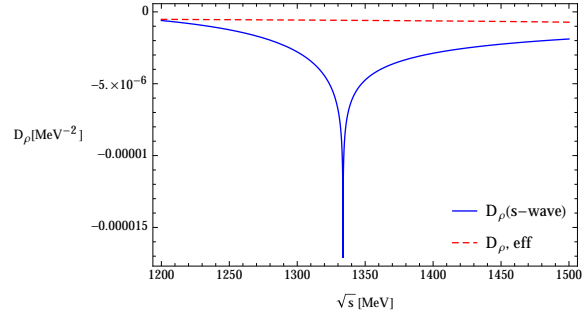


FIG. 10. Comparison of $D_{\rho,\text{eff}}$ of Eq. (18) evaluated with a cut off $q_{\text{max}} = 850$ MeV, and $D_{\rho}(s - \text{wave})$ of Eq. (7).

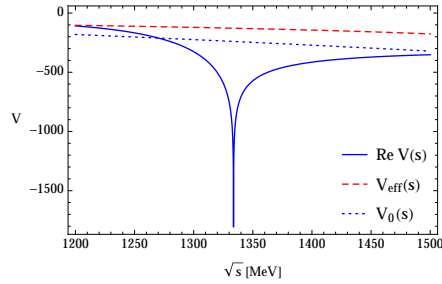


FIG. 11. Comparison of V_{eff} , $\text{Re } V(s)$ and the potential of [11].

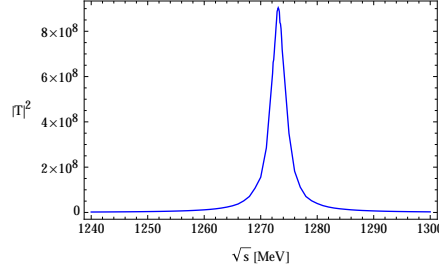


FIG. 12. $|T|^2$ evaluated with V_{eff} and \tilde{G} . The value of q_{max} is 1500 MeV.

and then V_{ex}/V_c is of the order of two. The strength of the two middle diagrams (b) and (c) of Fig. 8 will be about the same as in Fig. 8(d), actually even bigger when the loop is evaluated because of the reduction in the ρ propagator due to the explicit consideration of the full propagator. Then we concentrate on the diagram of Fig. 8(b) and evaluate it explicitly.

We want to see the difference between this diagram evaluated exactly and the same one when the ρ propagator is replaced by $-\frac{1}{M_\rho^2}$ as in [11].

In Fig. 9 we show explicitly the momenta of the variables. The loop function for this diagram considering only the propagators is given in the rest frame of the $\rho\rho$ system, $\vec{P} = 0$, by

$$t = i \int \frac{d^4 q}{(2\pi)^4} \frac{1}{(\frac{P^0}{2} - q^0)^2 - (\vec{p} - \vec{q})^2 - M_\rho^2 + i\epsilon} \frac{1}{2\omega(q)} \frac{1}{q^0 - \omega(q) + i\epsilon} \frac{1}{2\omega(q)} \frac{1}{(P^0 - q^0) - \omega(q) + i\epsilon} \quad (13)$$

with $\omega(q) = \sqrt{\vec{q}^2 + M_\rho^2}$, where we have kept the full ρ propagator for the exchanged ρ (including the energy dependence), but for the two intermediate ρ we keep their relativistic form but keeping only the positive energy part of the propagator since they will propagate close to on shell. There is practically no change from keeping the full propagators and the formulas are simplified, yet showing all the analytical structure. By performing analytically the q^0 integration in Eq. (13), we obtain

$$t = \int_{|\vec{q}| < q_{\text{max}}} \frac{d^3 q}{(2\pi)^3} \frac{1}{2\omega(q)^2} \frac{1}{2\omega(\vec{p} - \vec{q})} \frac{1}{P^0 - 2\omega(q) + i\epsilon} \frac{1}{\frac{P^0}{2} - \omega(q) - \omega(\vec{p} - \vec{q}) + i\epsilon}. \quad (14)$$

It is interesting to look at the analytical structure of the loop. We see two cuts, the one coming from $P^0 - 2\omega(q) + i\epsilon$ in the denominator, which corresponds to having the two intermediate ρ mesons on shell (the two lines in the diagrams of Fig. 9 cut by a vertical line) and from $\frac{P^0}{2} - \omega(q) - \omega(\vec{q} - \vec{q}) + i\epsilon$ in the denominator, which accounts for a possible situation where the exchanged ρ and one intermediate ρ are placed on shell. Yet, since $\omega(q) \geq M_\rho$, for a $\rho\rho$ system below threshold, where $P^0 < 2M_\rho$, this term never vanishes. We can, therefore, see that the exchanged ρ in the actual loops cannot produce any imaginary part, contrary to the “on shell” factorization of $V_\rho(s - \text{wave})$ of Eq. (7).

If one performs the same calculation with $-\frac{1}{M_\rho^2}$ for the exchanged ρ propagator we obtain

$$t_f = \int \frac{d^3 q}{(2\pi)^3} \left(-\frac{1}{M_\rho^2} \right) \frac{1}{4\omega(q)^2} \frac{1}{P^0 - 2\omega + i\epsilon}. \quad (15)$$

Comparing to t in Eq. (14) we see that we have replaced $\frac{1}{2\omega(\vec{p} - \vec{q})} \frac{1}{\frac{P^0}{2} - \omega(q) - \omega(\vec{p} - \vec{q})}$ by $\frac{-1}{2M_\rho^2}$, which holds exactly at threshold with $\vec{q} = \vec{p} - \vec{q} = 0$.

We can see that the explicit consideration of the propagator of the exchanged ρ has produced a reduction factor in the loop with respect to its replacement by $1/(-M_\rho^2)$ as in [11], but no singularities and no imaginary part. In view of this, one can anticipate that one would get similar results using the approach of [11] but using an explicit cut off that would effectively account for this converging factor. This means that if the cut off is fine tuned to obtain the peak of $|T|^2$ at the mass of the $f_2(1270)$ one will need a smaller q_{max} in the approach of [11] than using explicitly the loop evaluated here, that is formally convergent. We will come back to this point later on.

It is also interesting to note that

$$t_f \approx \left(-\frac{1}{M_\rho^2} \right) G \quad (16)$$

with G given by Eq. (2) by replacing

$$\frac{\omega_1 + \omega_2}{P^0{}^2 - (\omega_1 + \omega_2)^2 + i\epsilon} = \frac{1}{P^0 - \omega_1 - \omega_2 + i\epsilon} \frac{\omega_1 + \omega_2}{P^0 + \omega_1 + \omega_2} \approx \frac{1}{P^0 - \omega_1 - \omega_2 + i\epsilon} \frac{1}{2}. \quad (17)$$

In view of this, we define now an effective ρ -exchange in the following way

$$D_{\rho,\text{eff}} = \frac{t}{G(s)} \quad (18)$$

and hence we define an effective potential as

$$V_{\text{eff}} = V_c + (-M_\rho^2)V_{\text{ex}}D_{\rho,\text{eff}} \quad (19)$$

And now we will solve the Bethe Salpeter equation of Eq. (1). We can see that in the first loop including V_{ex} we would have

$$(-M_\rho^2)V_{\text{ex}}GD_{\rho,\text{eff}}V_c = (-M_\rho^2)V_{\text{ex}}V_c t. \quad (20)$$

Hence, by construction, with this effective potential and the Bethe Salpeter equation we are generating the exact loop that we have calculated. The term V_cGV_c of Fig. 8(a) does not experience any change with respect to [11] and in the term of Fig. 8(d) we would be making an approximation with respect to an exact evaluation of the loop with four propagators. It is possible to perform this loop exactly and we have done it. One can see a lengthy expression in Appendix C of [12]. Yet, the strength of this term is about one fourth of the total one loop contribution, as an average over q , and Eq. (16) is a sufficiently good approximation, even more when we know that small changes in a potential can be accommodated by small changes in the cut off of G , which is finally fitted to the precise mass of a state.

There is one more point to discuss. Indeed, the evaluation of t in Eq. (13) requires the knowledge of \vec{p} , the momentum of the initial ρ in the molecule that is finally formed. Only the modulus is needed since q is integrated over all angles and we can take \vec{p} in the z direction. In the “on shell” factorization \vec{p}^2 was negative. Taking \vec{p}^2 negative is one way to say that one has negative energies with respect to the threshold, and in this sense it is used when one looks for poles of the t -matrix below threshold. However, in the physical systems the momenta are certainly real. A bound state has negative energy and a wave function which corresponds to a distribution of real momenta. A very good approximation to the wave functions derived with a potential of the type $V\theta(q_{\text{max}} - q)\theta(q_{\text{max}} - q')$, which leads to the standard Bethe Salpeter equation with a cutoff q_{max} in the G function[18], is given in [18, 23]. Using Eqs. (105) of [23] and Eq. (47) of [18] we obtain

$$\langle p|\psi\rangle = g \frac{\theta(q_{\text{max}} - p)}{E - \omega_1(p) - \omega_2(p)} \quad (21)$$

where g is the coupling of the state to the components of the wave function ($\rho\rho$ in this case). We determine an average momentum by looking at the peak of $p^2\langle p|\psi\rangle^2$ and we find $p \approx 500$ MeV/c for $E = 1270$ MeV. This value could be smaller if the wave function picks up the lower components of the ρ mass distribution, but we take this value for the evaluation, and t is only smoothly dependent on p . For comparison p is of the order of 170 MeV/c for $E = 1500$ MeV.

In Fig. 10 we show the results for $D_{\rho,\text{eff}}(s)$ and compare it with $D_\rho(s - \text{wave})$ of Eq. (7). As one can see, there is a big difference between $D_{\rho,\text{eff}}$ and $D_\rho(s - \text{wave})$, the latter evaluated with the “on shell” factorization on top of the singularity.

In Fig. 11 we plot the effective potential V_{eff} of Eq. (19) as a function of the energy and compare it with the potential of [11] and from the “on shell” factorized potential, already shown in Fig. 3. As we can see, V_{eff} is smaller than the potential of [11], which is logical since it incorporates the q^2 dependence of the ρ propagator. Yet, the potential does not have any singularity, as is the case of $V(s)$, and we showed that the propagator in the loops does not develop a singularity. Also, V_{eff} below threshold does not have an imaginary part, unlike $V(s)$ which develops an imaginary part with a discontinuity at $s = 3M_\rho^2$.

In Fig. 12 we show now the results for $|T|^2$ using V_{eff} . As anticipated, in order to have a bound state at 1270 MeV, we must use now a larger value of q_{max} than in the case of the potential [11] because V_{eff} is already including effects of q^2 in the ρ propagator that reduces the contributions of the ρ exchange potential. Such effects are effectively taken into account in [11] by using a smaller cut off q_{max} . The calculation of Fig. 12 is done, as in Fig. 7, using the convoluted \tilde{G} function to account for the mass distribution of the ρ . The use of the convoluted \tilde{G} function in the Bethe Salpeter equation gives a width to the state because it can now decay to $\rho\pi\pi$ or $\pi\pi\pi\pi$. We already mentioned that this provides only part of the width. In the case of the $f_2(1270)$ most of the width comes from $\pi\pi$ decay, which

we evaluated in [11] by means of a box diagram. We refrain from doing it here, but the small width obtained using V_{eff} or the potential of [11] serves as the purpose of evaluating the coupling of the state to $\rho\rho$, which we do in the following way [13]

$$g_T^2 = M_R \Gamma_R \sqrt{|T|_{\text{max}}^2} \quad (22)$$

where M_R , Γ_R are the mass and width of the tensor state in Figs. 7 and 12 and $|T|_{\text{max}}^2$ is the value of $|T|^2$ at the peak. The value of g_T is $g_T = 10700 \text{ MeV}$ in the calculation with the effective potential and a cutoff 1500 MeV, and $g_T = 11700 \text{ MeV}$ with the potential of Ref. [11] and a cutoff 860 MeV. In both cases, the pole shows up at $\sqrt{s_0} = 1273 \text{ MeV}$ with a width of 3 MeV. If $p = 50 \text{ MeV}$ the pole with the effective potential appears at $\sqrt{s_0} = 1254 \text{ MeV}$, with $\Gamma = 2 \text{ MeV}$ and $g_T = 10000 \text{ MeV}$. While if $p = 800 \text{ MeV}$, we obtain the pole at $\sqrt{s_0} = 1300 \text{ MeV}$, with $\Gamma = 5 \text{ MeV}$ and $g_T = 11000 \text{ MeV}$.

We can see that the value of g_T is very similar in both approaches, with differences of less than 10%. This connects with our discussion in the Introduction because the compositeness condition [16–18] provides the coupling as a function of the binding energy for small binding, and in the present case, the fact that g_T is roughly model independent is somehow telling us that the wave function has picked up the low mass components of the ρ which provide less binding.

The fact that g_T is so stable and the results obtained are so close to those obtained before with the extreme approximation of neglecting the q^2 dependence of the ρ propagator, but coping for it by means of a reduced cut off, is very important and reinforces the agreement found with the couplings of [11] for the radiative decay of this resonance [13] and other decays [14].

V. CONCLUSIONS

We have made a critical discussion of a recent work [15] where certain improvements have been done in the $\rho\rho$ interaction. Yet, the use of the Bethe Salpeter equation with an “on shell” factorization of the potential leads the authors to conclude that, unlike the $f_0(1370)$ state, which appears as a bound $\rho\rho$ state, the tensor state $f_2(1270)$, which had been obtained before with some non relativistic approximations, disappears. We argue from a general point of view that if the potential for $J = 2$ is more than twice more attractive than the case of $J = 0$ (as is the case in [15]) and the $J = 0$ bound state is found in [15], the appearance of a bound state in $J = 2$ is unavoidable. Then we proceed to understand the reason of the claim in [15]. The problem stems from the “on shell” factorization of the potential on top of a singularity which produces a “potential” of infinite strength and with a big imaginary part that has a discontinuity in the singular point. We show that this imaginary part is unphysical and bears no connection to the decay products of the $\rho\rho$ bound state into $\pi\pi$ or $\pi\pi\pi\pi$. After the source of the anomalous results in [15] is disclosed, we proceed to tackle the problem in a realistic way, evaluating the loops with the full ρ propagators for the ρ in the exchange channel and see that there are no singularities nor an imaginary part below threshold tied to those diagrams. Finally, from the evaluated loops we define an effective potential in a way that when used with the Bethe Salpeter equation it renders the exact result of the loop. With this effective potential we solve the Bethe Salpeter equation and find a bound state for $J = 2$. Upon fine tuning of the cut off in the G function, taking into account the ρ mass distribution, the bound state is made to appear at 1270 MeV to generate the $f_2(1270)$ resonance, and its couplings to the $\rho\rho$ component is extracted. Then we find that the coupling evaluated with this improved method is very similar to the one obtained with a more drastic approximation done in [11], where in analogy to the construction of the chiral Lagrangians starting from the local hidden gauge Lagrangians, the q^2 in the propagators of the exchanged vector mesons is removed. We show that after tuning the cut off with this latter approximation, to approximately take into account the reduction of the exchanged propagators due to their q^2 dependence, and fitting the energy of the bound state to the experimental one, the resulting T matrix around the bound state energy is remarkably similar to the one obtained with the more sophisticated approach of the effective potential.

ACKNOWLEDGMENTS

This work is partly supported by the National Natural Science Foundation of China (Grants No.11375024 and No.11522539). This work is also partly supported by the Spanish Ministerio de Economía y Competitividad and European FEDER funds under the contract number FIS2011-28853-C02-01, FIS2011- 28853-C02-02, FIS2014-57026-REDT, FIS2014-51948-C2- 1-P, and FIS2014-51948-C2-2-P, and the Generalitat Valenciana in the program Prometeo II-2014/068. We acknowledge the support of the European Community-Research Infrastructure Integrating Activity Study of Strongly Interacting Matter (acronym HadronPhysics3, Grant Agreement n. 283286) under the Seventh

-
- [1] J. A. Oller and E. Oset, Nucl. Phys. A **620**, 438 (1997) Erratum: [Nucl. Phys. A **652**, 407 (1999)] [hep-ph/9702314].
 - [2] N. Kaiser, Eur. Phys. J. A **3**, 307 (1998).
 - [3] M. P. Locher, V. E. Markushin and H. Q. Zheng, Eur. Phys. J. C **4**, 317 (1998) [hep-ph/9705230].
 - [4] J. Nieves and E. Ruiz Arriola, Phys. Lett. B **455**, 30 (1999) [nucl-th/9807035].
 - [5] T. Waas, N. Kaiser and W. Weise, Phys. Lett. B **379**, 34 (1996).
 - [6] E. Oset and A. Ramos, Nucl. Phys. A **635**, 99 (1998) [nucl-th/9711022].
 - [7] J. A. Oller and U.-G. Meißner, Phys. Lett. B **500**, 263 (2001) [hep-ph/0011146].
 - [8] C. Garcia-Recio, J. Nieves, E. Ruiz Arriola and M. J. Vicente Vacas, Phys. Rev. D **67**, 076009 (2003) [hep-ph/0210311].
 - [9] T. Hyodo, S. I. Nam, D. Jido and A. Hosaka, Phys. Rev. C **68**, 018201 (2003) [nucl-th/0212026].
 - [10] J. A. Oller, E. Oset and A. Ramos, Prog. Part. Nucl. Phys. **45**, 157 (2000) [hep-ph/0002193].
 - [11] R. Molina, D. Nicmorus and E. Oset, Phys. Rev. D **78**, 114018 (2008) [arXiv:0809.2233 [hep-ph]].
 - [12] L. S. Geng and E. Oset, Phys. Rev. D **79**, 074009 (2009) [arXiv:0812.1199 [hep-ph]].
 - [13] H. Nagahiro, J. Yamagata-Sekihara, E. Oset, S. Hirenzaki and R. Molina, Phys. Rev. D **79**, 114023 (2009) [arXiv:0809.3717 [hep-ph]]; J. J. Xie, E. Oset and L. S. Geng, Phys. Rev. C **93**, 025202 (2016) [arXiv:1509.06469 [nucl-th]].
 - [14] E. Oset, L. S. Geng and R. Molina, J. Phys. Conf. Ser. **348**, 012004 (2012).
 - [15] D. Gülmez, U.-G. Meißner and J. A. Oller, arXiv:1611.00168 [hep-ph].
 - [16] S. Weinberg, Phys. Rev. **130**, 776 (1963). S. Weinberg, Phys. Rev. **137**, B672 (1965).
 - [17] V. Baru, J. Haidenbauer, C. Hanhart, Y. Kalashnikova and A. E. Kudryavtsev, Phys. Lett. B **586**, 53 (2004) [hep-ph/0308129].
 - [18] D. Gamermann, J. Nieves, E. Oset and E. Ruiz Arriola, Phys. Rev. D **81**, 014029 (2010) [arXiv:0911.4407 [hep-ph]].
 - [19] M. Bando, T. Kugo, S. Uehara, K. Yamawaki and T. Yanagida, Phys. Rev. Lett. **54**, 1215 (1985).
 - [20] M. Bando, T. Kugo and K. Yamawaki, Phys. Rept. **164**, 217 (1988).
 - [21] U.-G. Meißner, Phys. Rept. **161**, 213 (1988).
 - [22] J. A. Oller and E. Oset, Phys. Rev. D **60**, 074023 (1999) [hep-ph/9809337].
 - [23] J. Yamagata-Sekihara, J. Nieves and E. Oset, Phys. Rev. D **83**, 014003 (2011) [arXiv:1007.3923 [hep-ph]].